

Sulfonated hollow sphere carbon as an efficient catalyst for acetalisation of glycerol†

Cite this: *J. Mater. Chem. A*, 2013, **1**, 9422Received 6th March 2013
Accepted 26th April 2013

DOI: 10.1039/c3ta10956a

www.rsc.org/MaterialsA

Liang Wang,^{ab} Jian Zhang,^a Shuang Yang,^c Qi Sun,^a Longfeng Zhu,^b Qinming Wu,^a Haiyan Zhang,^b Xiangju Meng^a and Feng-Shou Xiao^{*a}

Sulfonated hollow sphere carbon (HSC-SO₃H) was synthesized from carbonization of a SiO₂-polymer core-shell structure, followed by removal of the SiO₂ core and sulfonation with chlorosulfonic acid. HSC-SO₃H shows superior performances in acetalisation of glycerol, which is related to the hollow sphere carbon shell with rich microporosity for good mass transfer in the reaction.

Biodiesel, which is regarded as a renewable fuel and has clear benefits relative to diesel fuel, has been widely produced from vegetable oils and animal fat.¹⁻⁴ In the production of biodiesel, glycerol is formed as a by-product in a large amount.¹⁻⁴ For example, 1.2 million tons of glycerol was formed in 2010, mostly coming from the production of biodiesel.⁴ Therefore, the conversion of glycerol into valuable chemicals has attracted much attention in recent years.⁵⁻⁷ Many routes have been developed to transform glycerol, such as hydrogenation, dehydration, dehydrogenation, esterification and oxidation.^{5,6} Particularly, acetalisation of glycerol with ketones or aldehydes is an efficient way to transform glycerol into important fine chemicals.⁷ For example, the acetalisation of glycerol with acetone could yield solketal (2,2-dimethyl-1,3-dioxolane-4-methanol, Scheme S1†), which could be directly applied as a fuel additive and surfactant.^{3b,7}

Normally, liquid acids and metal complexes show high catalytic activities in this kind of reaction, but these homogeneous catalysts have difficulty in separation and regeneration from the reaction system. Recently, the replacement of liquid acids by solid acids in acid-catalyzed reactions became a hot topic, due to the obvious advantages of heterogeneous catalysts including good stability and regenerability.⁸ Typically, aluminosilicate zeolites and sulfonated resins are two kinds of

heterogeneous solid acids.⁹ However, the small micropores of aluminosilicate zeolites strongly limit their use in the conversion of bulky molecules,^{9a} while the sulfonated resins with relatively low thermal stability are usually used at relatively low reaction temperatures.^{9c}

To overcome the low thermal stability of sulfonated resins, preparation of sulfonated carbons with relatively high thermal stability has been developed.^{2b,10,11} For example, Suganuma *et al.* reported that sulfonated amorphous carbon is catalytically active for hydrolysis of cellulose;^{11a,b} Wang *et al.* found that sulfated carbon could catalyze dehydration of fructose to 5-hydroxymethylfurfural (HMF).^{11c} Notably, most of the sulfated carbons have low surface areas due to the absence of porosity, which strongly limits the interaction between the acidic sites and substrates. Herein, we demonstrate a successful synthesis of sulfonated hollow sphere carbon (HSC-SO₃H) with a large surface area due to the hollow sphere structure with rich microporosity. As a typical model for glycerol conversion, catalytic tests in acetalisation of glycerol show that HSC-SO₃H exhibits high catalytic activity and excellent recyclability, compared with conventional solid acids. To the best of our knowledge, this is the first time that the acetalisation of glycerol is performed on porous carbon-based acids.

For the synthesis of HSC-SO₃H, resorcinol-formaldehyde resin and SiO₂ nanocomposites (SiO₂@resin) with a core-shell structure was synthesized under Stöber conditions at first.¹² After carbonization at 650 °C for 2 h, carbon and SiO₂ nanocomposites (SiO₂@HSC) were obtained. After washing with hydrofluoric acid, SiO₂ was removed and pure hollow sphere carbon (HSC) was obtained. Then, the HSC was treated with chlorosulfonic acid for 12 h at 0 °C, forming HSC-SO₃H (Scheme 1).

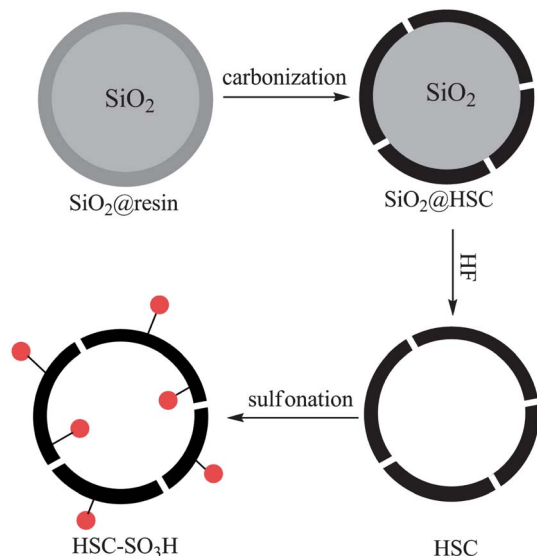
Fig. 1 shows TEM images of various samples. SiO₂@resin shows a typical core-shell structure (Fig. 1a). After carbonization, the sample morphology is still spherical (Fig. 1b). After removal of the silica core, a hollow sphere structure is clearly shown (Fig. 1c). The thickness of the carbon shell is about 10–13 nm, and the size of the hollow sphere is about 180–340 nm (Fig. 1d). In addition, a large scale SEM image indicates high purity of HSC (Fig. S1†).

^aKey Lab of Applied Chemistry of Zhejiang Province, Zhejiang University, Hangzhou 310028, China. E-mail: fsxiao@zju.edu.cn

^bState Key Laboratory of Inorganic Synthesis and Preparative Chemistry, Jilin University, Changchun 130012, China

^cDepartment of Chemistry, Jilin University, Changchun 130012, China

† Electronic supplementary information (ESI) available. See DOI: 10.1039/c3ta10956a



Scheme 1 Synthesis scheme of HSC-SO₃H (■ = resin, ■ = carbon, ● = -SO₃H).

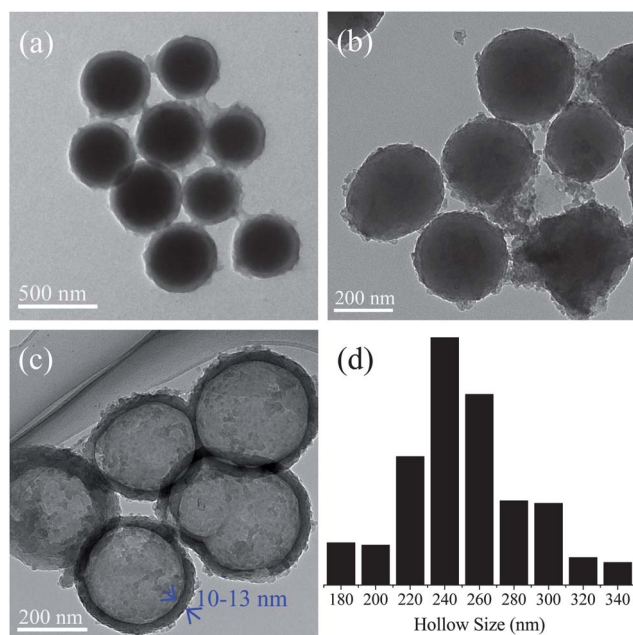


Fig. 1 TEM images of (a) SiO₂@resin, (b) SiO₂@HSC, and (c) HSC-SO₃H; (d) hollow size distribution of HSC-SO₃H.

Fig. 2A shows nitrogen sorption isotherms of SiO₂@resin and HSC-SO₃H. The SiO₂@resin sample exhibits low adsorption capacity for nitrogen and a very low surface area at 30 m² g⁻¹. However, HSC-SO₃H shows sorption isotherms of type IV plus type I. A steep increase occurs in the curve at a relative pressure of 10⁻⁶ < P/P₀ < 0.01, which is due to the filling of micropores (Fig. 2B).¹³ Density Functional Theory (DFT) micropore size distribution is estimated at 0.64 nm (Fig. 2C). The formation of micropores in the HSC-SO₃H is possibly attributed to the resin framework during the carbonization process. Another step can be identified in the curve at 0.85 < P/P₀ < 0.95, which is due to the presence of large pores.¹³ In this work, this feature should be

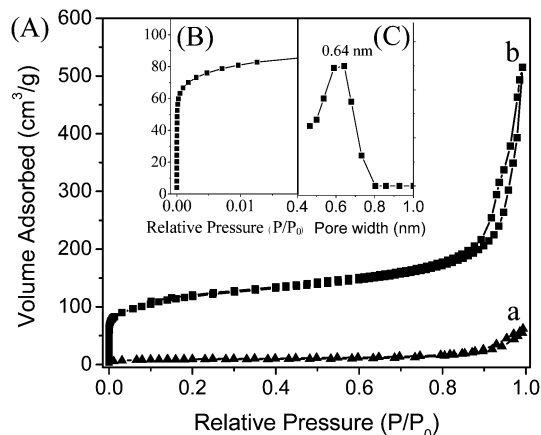


Fig. 2 (A) The nitrogen sorption isotherms of (a) SiO₂@resin and (b) HSC-SO₃H; (B) enlarged isotherms with a relative pressure of 10⁻⁶ to 0.01; (C) DFT micropore size distribution of HSC-SO₃H.

related to the hollow sphere structure. Very interestingly, the BET surface area of HSC-SO₃H is estimated at 419 m² g⁻¹. The large surface area of the sample is very helpful for catalytic conversion of glycerol because catalysis is a surface phenomenon.

Fig. 3 shows IR spectra of HSC and HSC-SO₃H. Compared with HSC, HSC-SO₃H shows obvious bands at 1031, 1119, and 1385 cm⁻¹. The band at 1031 cm⁻¹ is assigned to the presence of the C-S bond,¹⁴ while the bands at 1119 and 1385 cm⁻¹ are associated with the asymmetric and symmetric stretching signals of O=S=O bonds of a sulfonic group.¹⁴ These results indicate the successful introduction of sulfonic groups in the HSC-SO₃H sample.

Fig. 4 shows X-ray photoelectron spectra (XPS) of HSC-SO₃H. The survey spectrum gives signals mainly associated with C1s, O1s, and S2p species, indicating that HSC-SO₃H mainly consists of C, O, and S elements. Furthermore, the C1s XPS spectrum

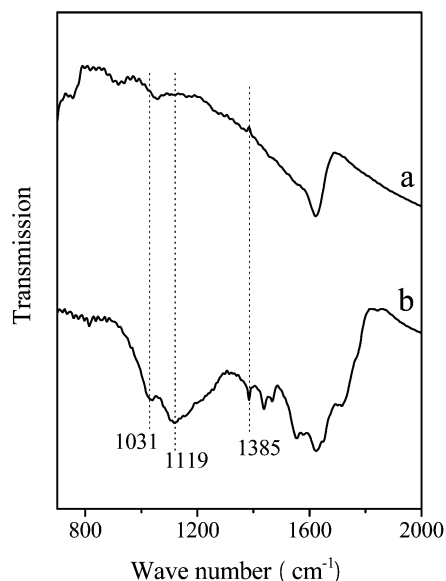


Fig. 3 IR spectra of (a) HSC and (b) HSC-SO₃H.

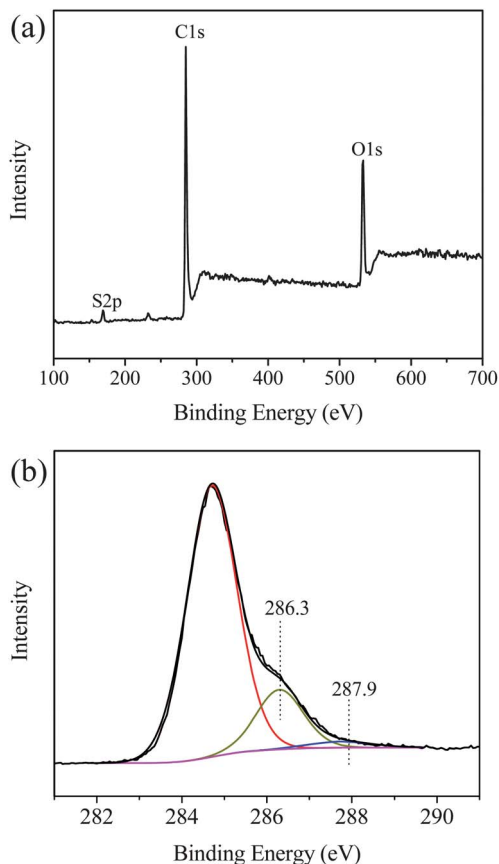


Fig. 4 (a) Survey and (b) C1s XPS spectra of HSC-SO₃H.

shows obvious signals at 286.3 and 287.9 eV, which are associated with C–S/C–O and C=O species. These results confirm the presence of sulfonic groups on HSC-SO₃H, which is in good agreement with those of IR spectra. Moreover, HSC-SO₃H gives an S2p peak at 169.1 eV (Fig. S2†), which is very similar to that of Amberlyst-15 (168.9 eV), suggesting that HSC-SO₃H and Amberlyst-15 have similar acidic strength of sulfonic groups, because the binding energy of S2p is sensitive to the acidic

strength.¹⁵ In addition, acid–base titration tests show that HSC-SO₃H has a relatively high acidic concentration at 1.9 mmol g^{−1}.

Fig. S3† shows TG curves of HSC-SO₃H and Amberlyst-15. Both curves show obvious weight loss at 40–165 °C, which is attributed to the desorption of water.¹⁶ Amberlyst-15 exhibits two weight losses centered at 309 and 455 °C, which are attributed to the decomposition of sulfonic groups and the Amberlyst-15 framework, respectively.¹⁶ In contrast, HSC-SO₃H requires a much higher temperature for the decomposition of sulfonic groups and the carbon framework at 388 and 512 °C, respectively. These results confirm that HSC-SO₃H has much better thermal stability than Amberlyst-15, which is very favorable for catalyst recycling.

Table 1 presents the catalytic data of various catalysts in acetalisation of glycerol. Solketal selectivity is greater than 98% in most of the cases. Notably, HSC without acidic groups results in very low conversion of glycerol (3.7%). However, after introduction of acidic sulfonic groups, HSC-SO₃H is very active, resulting in a conversion of 79.1% (entry 1, Table 1). This value is much higher than that of the homogeneous catalyst H₃PO₄W₁₂ (14.2%, entry 2, Table 1), heterogeneous catalysts SBA-15-SO₃H (44.5%, entry 3, Table 1), Amberlyst-15 (66.5%, entry 7, Table 1), H-USY zeolite (39.2%, entry 4, Table 1), and H-ZSM-5 zeolite (24.0%, entry 5, Table 1), and even comparable with that of liquid H₂SO₄ (82.8%, entry 8, Table 1).

Considering that Amberlyst-15 has a much higher acidic concentration than HSC-SO₃H and SBA-15-SO₃H has a much higher surface area than HSC-SO₃H, much higher activity over HSC-SO₃H than those over Amberlyst-15 and SBA-15-SO₃H should be related to the unique structure of hollow sphere carbon with rich microporosity. Possibly, the thin carbon shell (10–13 nm) with micropores is very favorable for mass transfer in acetalisation of glycerol. Therefore, most of the sulfonic groups inside and outside the hollow sphere carbon could be exposed to the reactants.¹⁷ In contrast, SBA-15-SO₃H and Amberlyst-15 have relatively long channels, resulting in relatively slow mass transfer.^{10b} As a consequence, some of the sulfonic groups on these porous catalysts might not be accessible to reactants.

Table 1 The textural, acidic parameters, and catalytic performances in acetalisation of glycerol and acetone to solketal over various acid catalysts^a

Entry	Catalysts	S content (mmol g ^{−1})	Acid density (mmol g ^{−1})	S _{BET} (m ² g ^{−1})	D _p ^b (nm)	Conversion ^c (%)
1	HSC-SO ₃ H	2.2	1.9	418	0.64	79.1 (78.5)
2	H ₃ PO ₄ W ₁₂		1.0	<5		14.2 (8.0)
3	SBA-15-SO ₃ H	1.2	1.1	815	7.3	44.5 (44.0)
4	H-USY ^d		2.0	610	0.72	39.2 (39.0)
5	H-ZSM-5 ^e		0.4	360	0.52	24.0 (23.7)
6	Sn-MCM-41		0.3 ^f	622	2.8	42.1 (42.0)
7	Amberlyst-15	4.0	4.3	46	39.5	66.5 (66.5) ^g
8	H ₂ SO ₄	10.2	20.4			82.8 (82.2) ^g
9 ^h	HSC-SO ₃ H	2.2	1.8	411	0.64	78.0 (78.0)
10 ^h	Amberlyst-15	3.8	3.8	37	42.2	57.4 (57.0)

^a Reaction conditions: 10 mmol of glycerol, 10 mmol of acetone, 4 g of *t*-BuOH, and 50 mg of catalyst with the temperature of oil bath at 80 °C for 6 h. ^b Average pore size distribution estimated from the DFT model for HSC-SO₃H and BJH model for other catalysts. ^c Glycerol conversion (solketal yield). ^d Ratio of Si/Al at 7.5. ^e Ratio of Si/Al at 40. ^f Sn density, ratio of Si/Sn at 50. ^g The same number of acidic sites as that of HSC-SO₃H in the reaction system. ^h Recycled for four times.

To investigate the mass transfer over the HSC-SO₃H catalyst, we performed the acetalisation reactions over HSC-SO₃H poisoned by pyridine and 4,4',4''-tris(2-methyl-2-propyl)-2,2':6',2''-terpyridine (tri-pyridine, Scheme S2†). When pyridine was added to the reaction system, HSC-SO₃H lost nearly all of its activity, because the small pyridine molecules could enter the hollow sphere carbon from the micropores, poisoning all acidic sites in and out of the hollow sphere carbon (Table S1, Scheme S2†). In contrast, when tri-pyridine was added to the reaction system, the poisoned HSC-SO₃H could still catalyze the acetalisation reaction, giving a glycerol conversion of 76.0% (Table S1†). This phenomenon is interpreted by the fact that the bulky tri-pyridine molecules could only poison the acidic sites on the outside surface of HSC-SO₃H due to the pore size limitation of the micropores (0.64 nm) on the carbon shell for the entrance of tri-pyridine. In this case, only acidic sites inside of the poisoned HSC-SO₃H could catalyze the acetalisation reaction. Furthermore, we performed the synthesis of the bulky molecule (2-(2-methoxyphenyl)-1,3-dioxolan-4-yl)-methanol by acetalisation of glycerol and 2-methoxybenzaldehyde (Scheme S3†). When pyridine or tri-pyridine was added to the reaction system, the HSC-SO₃H catalyst was nearly inactive (Table S2†), which is very different from the fact that only pyridine could make HSC-SO₃H lose all the activity in the acetalisation of glycerol and acetone (Table S1†). This phenomenon is due to the fact that the acetalisation of glycerol and 2-methoxybenzaldehyde only occurs on the external surface of HSC-SO₃H, because the micropores in HSC-SO₃H limit the transfer of the bulky molecule, the product (2-(2-methoxyphenyl)-1,3-dioxolan-4-yl)methanol (Scheme S4†). These observations, in particular the low activity in acetalisation of glycerol and 2-methoxybenzaldehyde over tri-pyridine-poisoned HSC-SO₃H, suggested that tri-pyridine almost completely poisoned all the acid sites on the external surface of HSC-SO₃H. Even if there were some acid sites which were not poisoned, they made almost no contribution to the catalytic acetalisation. Very interestingly, the conversion over the tri-pyridine poisoned HSC-SO₃H (76.0%, 100 mg catalyst) is very similar to that over as-synthesized HSC-SO₃H (79.1%, 50 mg catalyst); both catalysts have very similar turnover frequency (Table S1†). These results suggest that there is almost no limitation for mass transfer from the outside to inside of hollow sphere carbon. Additionally, these experiments also demonstrate that the pore size distribution of micropores in the hollow sphere carbon shell is ranged at kinetic diameters between pyridine and tri-pyridine because pyridine easily passes through the micropores and tri-pyridine is completely blocked by these micropores.

More importantly, HSC-SO₃H has excellent recyclability. For example, there is no obvious activity loss after recycling for 4 times (entries 1 and 9 in Table 1). In contrast, after the same number of recycles, glycerol conversion over the Amberlyst-15 catalyst decreased from 66.5 to 57.4% (entries 7 and 10 in Table 1). This phenomenon is due to leaching of acidic sites in Amberlyst-15 (entry 10 in Table 1). In contrast, acidic sites in HSC-SO₃H are relatively stable (entry 9 in Table 1), which is quite consistent with the results from TG analysis (Fig. S3†).

In summary, we have successfully prepared sulfonic groups functionalized hollow sphere carbon (HSC-SO₃H), which shows high activity and excellent recyclability in acetalisation of glycerol, compared with conventional solid acid catalysts. The superior catalytic performance is strongly related to the unique structure of sulfonated hollow sphere carbon with rich microporosity, which is favorable for mass transfer in the reaction. These features should be potentially important for the future design and synthesis of novel efficient catalysts for conversion of glycerol produced from biomass transformation.

Acknowledgements

This work is supported by the National Natural Science Foundation of China (21273197, and U1162201), State Basic Research Project of China (2009CB623501), National High-Tech Research and Development Program of China (2013AA065301), and Fundamental Research Funds for the Central Universities (2013XZZX001).

Notes and references

- (a) A. Corma, S. Iborra and A. Velty, *Chem. Rev.*, 2007, **107**, 2411; (b) C. H. C. Zhou, J. N. Beltramini, Y. X. Fan and G. Q. Lu, *Chem. Soc. Rev.*, 2008, **37**, 527; (c) A. Leonard, P. Dandoy, E. Danloy, G. Leroux, C. F. Meunier, J. C. Rooke and B.-L. Su, *Chem. Soc. Rev.*, 2011, **40**, 860.
- (a) A. Villa, J. P. Tessonnier, O. Majoulet, D. S. Su and R. Schlogl, *ChemSusChem*, 2010, **3**, 214; (b) M. Toda, A. Takagaki, M. Okamura, J. N. Kondo, S. Hayashi, K. Domen and M. Hara, *Nature*, 2005, **438**, 7065; (c) L. Xu, W. Li, J. Hu, K. Li, X. Yang, F. Ma, Y. Guo, X. Yu and Y. H. Guo, *J. Mater. Chem.*, 2009, **19**, 8571; (d) W. Li, Z. J. Jiang, F. Y. Ma, F. Su, L. Chen, S. Q. Zhang and Y. H. Guo, *Green Chem.*, 2010, **12**, 2135.
- (a) C.-H. Zhou, J. N. Beltramini, Y. X. Fan and G. Q. Lu, *Chem. Soc. Rev.*, 2008, **37**, 527; (b) L. Li, T. I. Koranyi, B. F. Sels and P. P. Pescarmona, *Green Chem.*, 2012, **14**, 1611; (c) D. M. Ladd, A. Volosin and D. K. Seo, *J. Mater. Chem.*, 2010, **20**, 5923; (d) F. Liu, L. Wang, Q. Sun, L. Zhu, X. Meng and F.-S. Xiao, *J. Am. Chem. Soc.*, 2012, **134**, 16948.
- (a) C. X. A. da Silva, V. L. C. Goncalves and C. J. A. Mota, *Green Chem.*, 2009, **11**, 38; (b) A. C. Pinto, L. N. Guarieiro, M. J. C. Resende, N. M. Ribeiro, E. A. Torres, W. A. Lopes, P. A. D. Pereira and J. B. Andrade, *J. Braz. Chem. Soc.*, 2005, **16**, 1313.
- (a) T. Miyazawa, Y. Kusunoki, K. Kunitomi and K. Tomishige, *J. Catal.*, 2006, **240**, 213; (b) E. P. Maris and R. J. Davis, *J. Catal.*, 2007, **249**, 328; (c) J. W. Shabaker, G. W. Huber and J. A. Dumesic, *J. Catal.*, 2004, **222**, 180; (d) Z. Q. Ma, Z. H. Xiao, J. A. van Bokhoven and C. H. Liang, *J. Mater. Chem.*, 2010, **20**, 755.
- (a) D. Wang, A. Villa, F. Porta, D. S. Su and L. Prati, *Chem. Commun.*, 2006, **18**, 1956; (b) L. Wang, W. Zhang, S. Zeng, D. S. Su, X. Meng and F.-S. Xiao, *Chin. J. Chem.*, 2012, **30**, 2189; (c) C. F. Meunier, P. Van Cusem, Y. U. Kwon and S.-L. Su, *J. Mater. Chem.*, 2009, **19**, 1535; (d) F. Wang, J. Xu, J. L. Dubois and W. Ueda, *ChemSusChem*, 2010, **3**, 1383.

- 7 (a) C. X. A. da Silva, V. L. C. Goncalves and C. J. A. Mota, *Green Chem.*, 2009, **11**, 38; (b) M. Rueping and V. B. Phapale, *Green Chem.*, 2012, **14**, 55; (c) G. Vicente, J. A. Melero, G. Morales, M. Paniagua and E. Martin, *Green Chem.*, 2010, **12**, 899; (d) P. Ferreira, I. M. Fonseca, A. M. Ramos, J. Vital and J. E. Castanheiro, *Appl. Catal., B*, 2010, **98**, 94; (e) C. J. Jia, Y. Liu, W. Schmidt, A.-H. Lu and F. Schuth, *J. Catal.*, 2010, **269**, 71.
- 8 (a) M. E. Davis, *Nature*, 2002, **417**, 813; (b) A. Corma, *Chem. Rev.*, 1995, **95**, 559; (c) D. E. De Vos, M. Dams, B. F. Sels and P. A. Jacobs, *Chem. Rev.*, 2002, **102**, 3615.
- 9 (a) F. Liu, T. Willhammar, L. Wang, L. Zhu, Q. Sun, X. Meng, W. Carrillo-Cabrera, X. Zou and F.-S. Xiao, *J. Am. Chem. Soc.*, 2012, **134**, 4557; (b) P. Barbaro and F. Liguori, *Chem. Rev.*, 2009, **109**, 515; (c) B. F. M. Kuster, *Starch/Staerke*, 1990, **42**, 314.
- 10 (a) M. Hara, T. Yoshida, A. Takagaki, T. Takata, J. N. Kondo, S. Hayashi and K. Domen, *Angew. Chem., Int. Ed.*, 2004, **43**, 2955; (b) F. Liu, J. Sun, L. Zhu, X. Meng, C. Qi and F.-S. Xiao, *J. Mater. Chem.*, 2012, **22**, 5495.
- 11 (a) S. Suganuma, K. Nakajima, M. Kitano, D. Yamaguchi, H. Kato, S. Hayashi and M. Hara, *J. Am. Chem. Soc.*, 2008, **130**, 12787; (b) K. Nakajima and M. Hara, *ACS Catal.*, 2012, **2**, 1296; (c) J. Wang, W. Xu, J. Ren, X. Liu, G. Lu and Y. Q. Wang, *Green Chem.*, 2011, **13**, 2678.
- 12 (a) W. Stober, A. Fink and E. Bohn, *J. Colloid Interface Sci.*, 1968, **26**, 62; (b) A. B. Fuertes, P. Valle-Vigon and M. Sevilla, *Chem. Commun.*, 2012, **48**, 6124.
- 13 R. Xu, W. Pang, J. Yu, Q. Huo and J. Chen, *Chemistry of Zeolite and Related Porous Materials*, Wiley, Singapore, 2007.
- 14 (a) F. Liu, W. kong, C. Qi, L. Zhu and F.-S. Xiao, *ACS Catal.*, 2012, **32**, 565; (b) R. Xing, N. Liu, Y. M. Liu, H. H. Wu, Y. W. Jiang, L. Chen, M. Y. He and P. Wu, *Adv. Funct. Mater.*, 2007, **17**, 2455.
- 15 (a) A. K. Geim, *Science*, 2009, **324**, 1530; (b) K. S. Noveselov, A. K. Geim, S. V. Morozov, D. Jiang, Y. Zhang, S. V. Dubonos, I. V. Grigorieva and A. A. Firsov, *Science*, 2004, **306**, 666; (c) K. S. Noveselov, A. K. Geim, S. V. Morozov, D. Jiang, M. I. Katsnelson, I. V. Grigorieva, S. V. Dubonos and A. A. Firsov, *Nature*, 2005, **438**, 197.
- 16 (a) N. Bother, F. Descher, J. Klein and H. Widdecke, *Polymer*, 1979, **20**, 850; (b) H. Widdecke, *Br. Polym. J.*, 1984, **16**, 188.
- 17 S. Suganuma, K. Nakajima, M. Kitano, H. Kato, A. Tamura, H. Kondo, Yanagawa, S. Hayashi and M. Hara, *Microporous Mesoporous Mater.*, 2011, **443**, 143.